Published paper

Quilter, J.H., Brash, A.J., Liu, F., Glaessl, M., Barth, A.M., Axt, V.M., Ramsay, A.J., Skolnick, M.S. and Fox, A.M. (2015) *Phonon-Assisted Population Inversion of a Single InGaAs/GaAs Quantum Dot by Pulsed Laser Excitation*. Physical Review Letters, 114 (13)

10.1103/PhysRevLett.114.137401

Phonon-assisted population inversion of a single InGaAs/GaAs quantum dot by pulsed laser excitation

J. H. Quilter,[1] A. J. Brash,[1] F. Liu,[1,*] M. Glässl,[2] A. M. Barth,[2]
V. M. Axt,[2] A. J. Ramsay,[3] M. S. Skolnick,[1] and A. M. Fox[1]

[1]*Department of Physics and Astronomy, University of Sheffield, Sheffield, S3 7RH, United Kingdom*
[2]*Institut für Theoretische Physik III, Universität Bayreuth, 95440 Bayreuth, Germany*
[3]*Hitachi Cambridge Laboratory, Hitachi Europe Ltd., Cambridge CB3 0HE, United Kingdom*
(Dated: February 3, 2015)

We demonstrate a new method to realize the population inversion of a single InGaAs/GaAs quantum dot excited by a laser pulse tuned within the neutral exciton phonon sideband. In contrast to the conventional method of inverting a two-level system by performing coherent Rabi oscillation, the inversion is achieved by rapid thermalization of the optically dressed states via incoherent phonon-assisted relaxation. A maximum exciton population of 0.67 $\pm$ 0.06 is measured for a laser tuned 0.83 meV to higher energy. Furthermore, the phonon sideband is mapped using a two-color pump-probe technique, with its spectral form and magnitude in very good agreement with the result of path-integral calculations.

It is a basic tenet of laser physics that a population inversion cannot be achieved through incoherent excitation of a two-level atom. At best, a laser pulse with duration much longer than the coherence time of the two-level system T_2 can only drive the system to the transparency point where the populations of the upper and lower levels are equal[1]. However, if the two-level atom is coupled to a vibrational continuum, it has been predicted that inversion can be possible even in the incoherent regime through the interaction of the dressed states with the Boson bath[2]. Excitons in semiconductor quantum dots (QDs) form a near ideal system for investigating these effects, since their behavior approximates well to that of a two-level atom[3], while their coupling to the acoustic phonons in the crystal provides a mechanism to thermalize the dressed states.

The possibility of creating population inversion in QDs through phonon coupling was first investigated for microwave-driven electrostatic quantum dots[4]. Recently, it has been demonstrated that the conditions for population inversion can be met via a microwave Raman effect [5, 6]. Theoretical work has indicated that similar effects should be possible for optically-driven excitons [7–11]. The underlying mechanism is the coupling of the excitons to longitudinal acoustic (LA) phonons through the deformation potential [12], which generates sidebands in the excitonic spectra [13] that can also be observed in four-wave mixing[14] and resonance fluorescence experiments[15], as well as through off-resonant coupling of excitons to nano-cavities[16, 17]. In a strong driving field regime, evidence for phonon induced relaxation between optically dressed states is observed in the intensity damping of Rabi rotations [18–20], and more recently in adiabatic rapid passage experiments [21, 22].

In this Letter we report a population inversion of the excitonic two-level system of a single InGaAs/GaAs QD excited by a strong laser pulse tuned into the phonon sideband of the neutral exciton transition following the theoretical proposal of Ref. [9]. The population inversion is achieved in an incoherent regime where the dephasing time is shorter than the laser pulse duration. Pump-probe measurements are presented, where the phonon-assisted population inversion is observed clearly as a gain-like dip in the photocurrent absorption spectrum. Furthermore, the dependence of the exciton population on the pump detuning is measured. The experiments are supplemented by simulations based on the path-integral approach described in Ref. [23] and good agreement is obtained with the theory. This work may form the basis of quasi-resonantly pumped single QD lasers. It also shows that the phonon-assisted quasi-resonant excitation scheme can be used to create spin-polarized excitons whilst allowing the QD emission to be spectrally filtered from the pump laser, with potential applications for QD-based high-brightness single photon sources [17] and on-chip quantum optical circuits [24].

The physical mechanism for generating the population inversion can be understood as follows. A circularly-polarized laser pulse with a large pulse area excites the neutral exciton transition of an InGaAs/GaAs quantum dot at a positive detuning within the phonon-sideband, which typically peaks around 1 meV above the exciton (see Fig. 4(a) insert). Since the laser bandwidth of 0.2 meV is large compared with the fine-structure splitting of 13 μeV, the dynamics of the exciton spin can be neglected[25]. Also, since the laser is far detuned from the two-photon biexciton transition, the QD can be treated as a two-level system composed of two bare states: a crystal ground-state $|0\rangle$, and neutral exciton $|X\rangle$ (see Fig. 1(a)(i)), with respective populations: C_0 and C_X. With the presence of a laser pulse, the two bare states are optically dressed (see Fig. 1(a)(ii), (iii)). In the rotating frame, $|0_{\rm R}\rangle$ comprises the crystal ground state and the incoming laser photons. $|X_{\rm R}\rangle$ comprises the exciton state and laser field with one photon less.

The Hamiltonian in a rotating frame reads:

$$H_{\mathrm{QD}} = -\hbar\Delta|X_{\mathrm{R}}\rangle\langle X_{\mathrm{R}}| + \frac{\hbar\Omega(t)}{2}|0_{\mathrm{R}}\rangle\langle X_{\mathrm{R}}| + H.c., \quad (1)$$

where the detuning $\Delta = \omega_{\mathrm{L}} - \omega_X$, and $\Omega(t)$ is the Rabi frequency, which varies in time following the envelope of the laser pulse. The energy eigenstates of H_{QD}, $|\alpha\rangle$, $|\beta\rangle$ are described by an admixing angle $2\theta(t) = \arctan(\Omega(t)/\Delta)$, and are split by the effective Rabi energy $\hbar\Lambda(t) = \hbar\sqrt{\Delta^2 + \Omega(t)^2}$. We define the bare pulse area $\Theta = \int_{-\infty}^{+\infty} \Omega(t)\,\mathrm{d}t$.

The QD resides in a crystal lattice, and the exciton interacts with the LA phonons due to the deformation potential [12]. In the absence of a laser-field, the exciton-phonon interaction leads to non-exponential pure-dephasing of the excitonic dipole, as observed in time-resolved four-wave mixing experiments [14]. In the presence of a strong laser, both dressed states have an excitonic component, thereby enabling relaxation between them by the emission of a phonon with energy equal to the effective Rabi-splitting $\hbar\Lambda$, as shown in Fig. 1(a)(iii) for the case of positive detuning. This process gives rise to intensity damping of Rabi rotations when resonantly pumping [18, 19], and also explains the difference in the population inversions created by adiabatic rapid passage when using laser pulses of positive and negative chirp [21, 22].

Figure 1(b) depicts the dynamics in the rotating frame of the phonon-assisted population inversion of the quantum dot exciton. For a positively detuned laser ($\Delta > 0$), the state $|0_{\mathrm{R}}\rangle$ initially coincides with the higher-energy dressed state $|\alpha\rangle$. When the laser is applied, excitonic admixture to the state $|\alpha\rangle$ occurs, activating relaxation to the lower-energy dressed state $|\beta\rangle$ by phonon emission. In the lab frame (see Fig. 1(a)(i)), this process corresponds to the absorption of a photon together with the creation of an exciton and the emission of a phonon. The greyscale indicates the time-dependent populations of each dressed state, as calculated by our path-integral method, and shows the continuous transfer of population from $|\alpha\rangle$ to $|\beta\rangle$. As the laser intensity drops off at the end of the pulse, the admixing of the dressed states is reduced and the phonon relaxation is deactivated. If the time-integrated phonon-relaxation is strong, the final occupation of the lower-energy, exciton-like, dressed state can dominate and a population inversion in the excitonic basis occurs. According to our theoretical model, near-unity exciton population that is robust against variations in both the pulse-area and the detuning can be achieved at high pulse-areas [9]. The amount of inversion is ultimately limited by the thermal occupation of the two states to $C_X - C_0 = \tanh(\hbar\Delta/2k_{\mathrm{B}}T)$ [9]. In our experiments with $\hbar\Delta = 0.83$ meV and $T = 4.2$ K, this implies a maximum exciton population of 0.91.

The experiments were performed on a device consisting of a layer of InGaAs/GaAs quantum dots embedded in

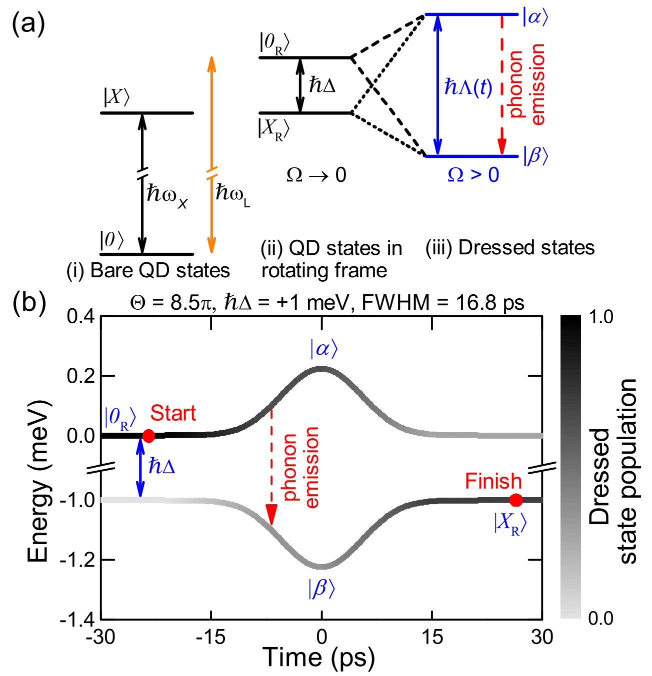

FIG. 1. Color online. (a) Bare QD states viewed in the (i) lab frame and (ii) rotating frame. $|0\rangle$, $|X\rangle$ and $|0_{\mathrm{R}}\rangle$, $|X_{\mathrm{R}}\rangle$ denote the ground state and exciton state in the lab frame and rotating frame respectively. $\hbar\omega_X$ is the exciton transition energy. ω_{L} is the angular frequency of the laser. $\hbar\Delta$ is the positive detuning from the exciton transition. (iii) Optically dressed states $|\alpha\rangle$ and $|\beta\rangle$. (b) Evolution of the dressed QD energy levels with time during the absorption of an 8.5π pulse with $\hbar\Delta = +1$ meV. The greyscale of the curves corresponds to the instantaneous population of each state.

the intrinsic region of an n-i-Schottky diode structure. The sample is held at 4.2 K in a helium bath cryostat and is excited at normal incidence with circularly polarized Gaussian pulses, derived by pulse-shaping of the output from a 100 fs Ti:sapphire laser with repetition rate of 76.2 MHz. The FWHM of the electric field amplitude is 16.8 ps. Single QD peaks are observed in our sample at energies close to 1.3 eV. Photocurrent detection is used, where photo-generated electron-hole pairs tunnel from the quantum dot under an applied electric-field. The amplitude of the photocurrent signal reflects the final occupation of the exciton or biexciton states. Full details of the wafer structure can be found in Ref. 26.

To demonstrate the phonon-assisted population inversion, two-pulse pump probe experiments were performed. First, the zero-phonon neutral exciton transition was found by measuring the absorption spectrum of a single π-pulse (blue line in Fig. 2). Then the pump pulse was detuned by $+0.83$ meV, where the exciton population is predicted to be most efficiently created (see blue line in Fig. 4(a)), and the probe energy is scanned through the transition. The probe pulse area is π and the pump pulse area is 8.46π, the maximum available in our setup.

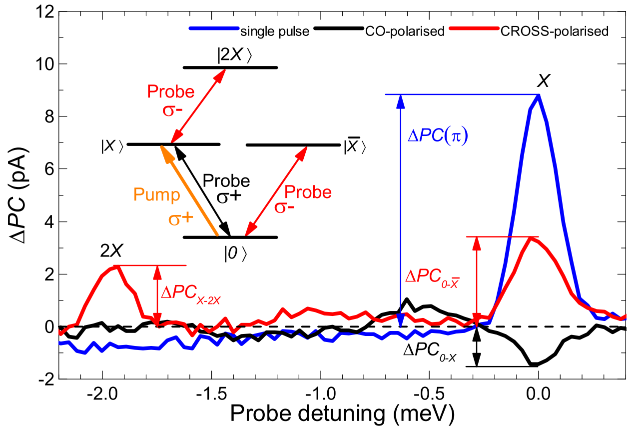

FIG. 2. Color online. Photocurrent signal ΔPC as a function of the probe detuning. (Blue) A single probe-pulse only spectrum is presented for reference. Two pulse spectra where the probe is co- (black) and cross- (red) polarized with the pump. Pump detuning = +0.83 meV and $\tau_{\text{delay}} = 10$ ps. The peak at a detuning of -1.96 meV corresponds to the $|X\rangle \rightarrow |2X\rangle$ transition. Insert: energy level diagram for the exciton-biexciton system. Arrows represent transitions induced by the σ^+ polarized pump pulse tuned to the phonon sideband and the σ^+/σ^- polarized probe pulse tuned either to the exciton or biexction transition. X and $\bar{X}$ label the orthogonally circularly polarised exciton states. $2X$ denotes the biexciton state.

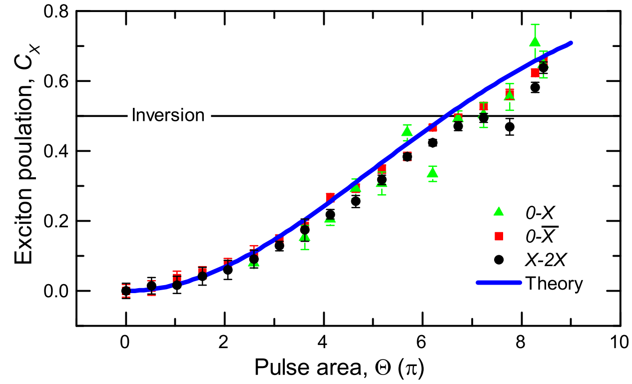

FIG. 3. Color online. The exciton population C_X generated by the pump pulse with $\hbar\Delta = +0.83$ meV, as extracted from the exciton and biexciton peak in two-pulse spectra versus the pump pulse area. For a full derivation, see [27]. (Blue) Calculated C_X.

The delay time between the pump and probe pulses τ_{delay} ranges from 10 to 34 ps [27].

As illustrated in the energy-level diagram shown in Fig. 2, the photon energy of the probe pulse and its polarization relative to the pump selects the transition that is probed. We consider first the case for a co-polarized probe pulse, where both the pump and probe pulses have the same σ^+-polarization. In this case, the pump pulse (orange arrow) excites a dephased, mixed exciton population C_X (see the insert in Fig. 2). Since the probe has a pulse area of π, it exchanges the $|0\rangle$ population with the $|X\rangle$ population when it is resonant with the neutral exciton transition (see black arrow in the insert to Fig. 2), resulting in a change in photocurrent proportional to the populations after the pump but before the probe: $\Delta PC_{0-X} \propto C_0 - C_X$ [27]. ΔPC is the change in the photocurrent signal resulting from the dot that is induced by the probe pulse. ΔPC is measured relative to the photocurrent measured for a detuned probe. A key signature of population inversion is that ΔPC_{0-X} should be negative, independent of the photocurrent to exciton population calibration. Figure 2 shows the experimental results (black). The dip at zero-detuning clearly demonstrates that a population inversion has been achieved between the $|0\rangle$ and $|X\rangle$-states.

The red line in Fig. 2 shows the results obtained for cross-polarized excitation (σ^+ pump, σ^- probe). At zero-detuning, the probe addresses the orthogonally polarized exciton transition $|0\rangle \rightarrow |\bar{X}\rangle$ as shown by the lower red arrow in the insert to Fig. 2, providing a measure of the occupation of the crystal ground-state C_0. The amplitude of the peak at zero detuning falls to less than half the amplitude measured by the single pulse, again confirming that a population inversion between $|0\rangle$ and $|X\rangle$ has been achieved since $\Delta PC_{0-\bar{X}} \propto C_0 - C_{\bar{X}}$. The second peak at a detuning of -1.96 meV corresponds to the $|X\rangle \rightarrow |2X\rangle$ transition, and provides a third measure of C_X (see [27]). The absence of the biexciton peak in the co-polarized spectra proves that the phonon-assisted channel is spin-preserving because the phonon-assisted relaxation (few ps) [28] is much faster than exciton spin relaxation (few ns) [29].

Figure 3 plots the occupation of the neutral exciton versus the area of the pump pulse. The three data points for each pulse area are obtained from an analysis of the co- and cross-polarized signals at zero detuning, and from the biexciton peak. The exciton population is deduced by comparison with the neutral exciton photocurrent peak for resonant excitation with a single π-pulse (for details, see [27]). Since the electron can tunnel out from the QD before the arrival of the probe, which reduces the measured exciton population created by the pump, a correction is made to account for an electron tunneling time of $\sim$50 ps [27]. The three measurements of the exciton population are in close agreement, and pass the transparency point, $C_X = 0.5$, at a pulse-area of $6.5 - 7\pi$. The largest exciton population observed is 0.67 ± 0.06 for a pump pulse detuned by +0.83 meV, limited by the power available in our setup. The blue line in Fig. 3 shows the results of our path-integral simulations which quantitatively reproduce the experiments.

To investigate the dependence of the phonon-assisted population inversion on the pump frequency, a series of two-color photocurrent spectra, similar to Fig. 2,

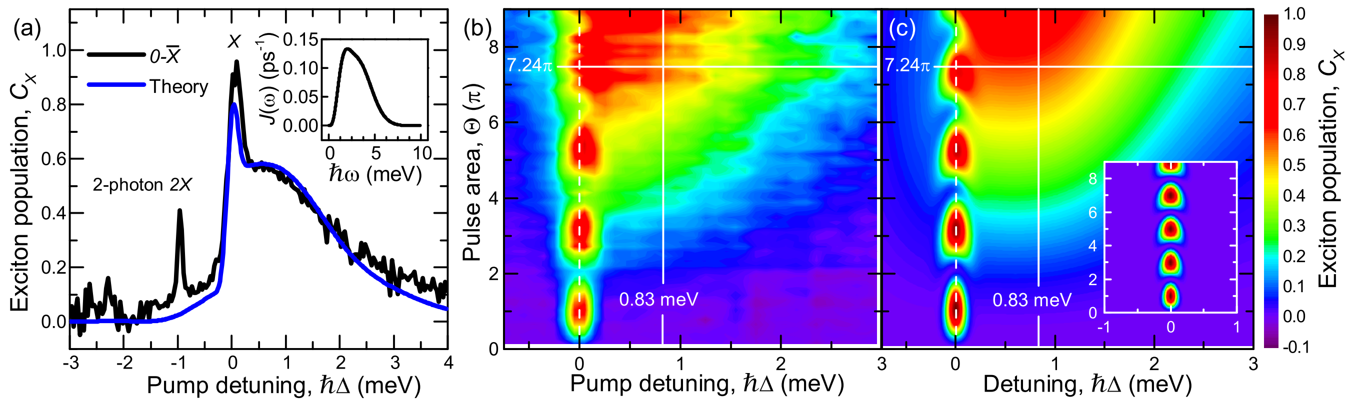

FIG. 4. Color online. (a) Exciton population created by a 7.24π pump as a function of the pump detuning. $\tau_{\rm delay} = 15$ ps. Blue: Calculated C_X. Insert: Theoretical spectral density of the exciton-phonon interaction $J(\omega)$. (b) Experimentally obtained C_X vs Θ and $\hbar\Delta$ with $\tau_{\rm delay} = 33.6$ ps. (c) Path-integral results for the same pulse area and detuning range as in (b). The vertical line is where $\hbar\Delta = +0.83$ meV and horizontal line is for $\Theta = 7.24\pi$ as shown in Figs. 3 and 4(a), respectively. Inset: calculated values with no phonon interaction. All plots in (b) and (c) use the same colour scale.

were measured for a cross-polarized 7.24π pump pulse as a function of pump detuning with a π probe. Figure 4(a) presents the exciton population generated by the pump pulse. The spectrum has three features. At zero-detuning there is a pulsewidth-limited peak corresponding to the zero-phonon $|0\rangle \rightarrow |X\rangle$ transition. At positive detuning there is a broad feature due to phonon emission. The absence of discrete features in the phonon sideband indicates that phonon confinement effects are weak, as expected given the similar lattice properties of the QD and barrier materials. In principle, there can also be a phonon feature at negative detuning due to phonon absorption. However, the phonon absorption is negligible at low temperature. The third feature is a narrow peak at a pump detuning of -1 meV, corresponding to the two-photon $|0\rangle \rightarrow |2X\rangle$ biexciton transition[30], indicating that the pump pulse is slightly elliptically polarized.

In the theory, the phonon influence on the dot dynamics is mediated mainly by the phonon spectral density: $J(\omega) = \sum_{\mathbf{q}} |\gamma_{\mathbf{q}}|^2 \, \delta(\omega - \omega_{\mathbf{q}})$, where $\gamma_{\mathbf{q}}$ is the exciton-phonon coupling. In the absence of detailed information on the shape of the QD we consider spherically symmetric, parabolic potentials. For bulk LA phonons coupled via the deformation potential we then obtain[23]:

$$J(\omega) = \frac{\omega^3}{4\pi^2 \rho \hbar v_c^5} \left[D_{\rm e} \, e^{\left(-\omega^2 a_{\rm e}^2/4v_c^2\right)} - D_{\rm h} \, e^{\left(-\omega^2 a_{\rm h}^2/4v_c^2\right)} \right]^2 , \tag{2}$$

where ρ is the mass density, v_c the sound velocity and $D_{\rm e/h}$ denote the deformation potential constants for electrons and holes. These material parameters are taken from the literature and are given explicitly in the supplement [27], while the electron and hole confinement lengths $a_{\rm e/h}$ are used as fitting parameters. Good agreement with our experiments is obtained for $a_{\rm e} = 4.5$ nm and $a_{\rm h} = 1.8$ nm resulting in the spectral density shown in the insert of Fig. 4(a). We note that the low frequency asymptote $\sim \omega^3$ is characteristic for bulk acoustic phonons and occurs independent of the material or the dot shape. On the other hand, the Gaussians in Eq. (2) result from the Fourier transforms of the electron and hole probability densities, reflecting the assumption of parabolic confinement potentials.

The blue line in Fig. 4(a) shows the theoretical values of the exciton population generated by the pump pulse, which excellently replicates the broadband feature observed at positive detuning. The lineshape of this feature is implicitly determined by $J(\omega)$; more detailed information on $J(\omega)$ can be obtained here than from fitting the intensity damping of Rabi rotations [19]. Eq. (2) shows that high frequency behavior of $J(\omega)$ follows the Fourier transform of the electron and hole probability densities, and so a lineshape analysis in principle provides a way to obtain insight on the spatial distributions of the electrons and holes. However, accessing this information would require more detailed studies which are beyond the scope of the present Letter. The asymmetry of the spectrum with respect to the sign of $\hbar\Delta$ unambiguously proves that the population created by the off-resonant pump pulse is the result of phonon-assisted relaxation into the lower energy dressed state[31]. This is further demonstrated by a calculation without exciton-phonon coupling, where no broad sideband is observed (see insert in Fig. 4(c)). We also note that the measured low-energy phonon sideband is stronger than expected. This may be due to an elevated temperature of about 6-7 K caused by heating of the sample by the laser.

Figures 4(b) and (c) compare the exciton population generated by the pump pulse measured as in Fig. 4(a) at different pulse areas with corresponding path-integral calculations. On-resonance, the zero-phonon line exhibits intensity-damped Rabi rotations. To positive detuning, there is the phonon-emission sideband that broadens for higher pulse areas. The calculations are in good agreement with the experimental data, further confirming the model. Even the slight shift of the resonant peaks towards higher energies with increasing pulse area is reproduced by the theory.

In conclusion, we have experimentally demonstrated the population inversion of a neutral exciton in a single QD excited by a quasi-resonant laser pulse tuned within the exciton phonon sideband. The population inversion arises due to incoherent phonon-induced relaxation between optically dressed states which arises at high driving intensities. Phonon interactions, which are usually a hindrance in quantum dot physics, in this case enable the population inversion and lead to qualitatively distinct behaviour. The phonon-mediated population inversion we report may have potential as the basis of quasi-resonantly pumped single QD lasers with dots embedded in cavities, and as high repetition rate single photon sources [17], with easy spectral filtering of excitation lasers, especially relevant to on-chip geometries [24].

This work was funded by the EPSRC (UK) EP/J007544/1. MG, AMB and VMA gratefully acknowledge the financial support from Deutsche Forschungsgemeinschaft via the project AX 17/7-1. The authors thank H. Y. Liu and M. Hopkinson for sample growth.

* email: fengliu@sheffield.ac.uk

[1] A. E. Siegman, *Lasers* (University Science Books, Oxford, 1986).

[2] A. J. Leggett, S. Chakravarty, A. T. Dorsey, M. P. A. Fisher, A. Garg, and W. Zwerger, Rev. Mod. Phys. **59** (1987).

[3] T. Stievater, X. Li, D. Steel, D. Gammon, D. Katzer, D. Park, C. Piermarocchi, and L. Sham, Phys. Rev. Lett. **87**, 133603 (2001).

[4] J. Petta, A. Johnson, C. Marcus, M. Hanson, and A. Gossard, Phys. Rev. Lett. **93**, 186802 (2004).

[5] T. M. Stace, A. C. Doherty, and S. D. Barrett, Phys. Rev. Lett. **95**, 106801 (2005).

[6] J. I. Colless, X. G. Croot, T. M. Stace, A. C. Doherty, S. D. Barrett, H. Lu, A. C. Gossard, and D. J. Reilly, Nat. Commun. **5**, 3716 (2014).

[7] M. Glässl, A. Vagov, S. Lüker, D. E. Reiter, M. D. Croitoru, P. Machnikowski, V. M. Axt, and T. Kuhn, Phys. Rev. B **84**, 195311 (2011).

[8] D. E. Reiter, S. Lüker, K. Gawarecki, A. Grodecka-Grad, P. Machnikowski, V. M. Axt, and T. Kuhn, Acta Phys. Pol. A **122**, 1065 (2012).

[9] M. Glässl, A. M. Barth, and V. M. Axt, Phys. Rev. Lett. **110**, 147401 (2013).

[10] S. Hughes and H. J. Carmichael, New J. Phys. **15**, 053039 (2013).

[11] D. E. Reiter, T. Kuhn, M. Glässl, and V. M. Axt, Journal of physics. Condensed matter **26**, 423203 (2014).

[12] B. Krummheuer, V. Axt, and T. Kuhn, Phys. Rev. B **65**, 195313 (2002).

[13] L. Besombes, K. Kheng, L. Marsal, and H. Mariette, Phys. Rev. B **63**, 155307 (2001).

[14] P. Borri, W. Langbein, U. Woggon, V. Stavarache, D. Reuter, and A. Wieck, Phys. Rev. B **71**, 115328 (2005).

[15] S. Weiler, A. Ulhaq, S. M. Ulrich, D. Richter, M. Jetter, P. Michler, C. Roy, and S. Hughes, Phys. Rev. B **86**, 241304 (2012).

[16] U. Hohenester, A. Laucht, M. Kaniber, N. Hauke, A. Neumann, A. Mohtashami, M. Seliger, M. Bichler, and J. J. Finley, Phys. Rev. B **80**, 201311 (2009).

[17] K. H. Madsen, S. Ates, J. Liu, A. Javadi, S. M. Albrecht, I. Yeo, S. Stobbe, and P. Lodahl, Physical Review B **90**, 155303 (2014).

[18] A. J. Ramsay, A. V. Gopal, E. M. Gauger, A. Nazir, B. W. Lovett, A. M. Fox, and M. S. Skolnick, Phys. Rev. Lett. **104**, 017402 (2010).

[19] A. J. Ramsay, T. M. Godden, S. J. Boyle, E. M. Gauger, A. Nazir, B. W. Lovett, A. M. Fox, and M. S. Skolnick, Phys. Rev. Lett. **105**, 177402 (2010).

[20] L. Monniello, C. Tonin, R. Hostein, A. Lemaitre, A. Martinez, V. Voliotis, and R. Grousson, Physical Review Letters **111**, 026403 (2013).

[21] Y.-J. Wei, Y.-M. He, M.-C. Chen, Y.-N. Hu, Y. He, D. Wu, C. Schneider, M. Kamp, S. Höfling, C.-Y. Lu, et al., arXiv (2014), arXiv:1405.1991.

[22] R. Mathew, E. Dilcher, A. Gamouras, A. Ramachandran, H. Y. S. Yang, S. Freisem, D. Deppe, and K. C. Hall, Physical Review B **90**, 035316 (2014).

[23] A. Vagov, M. D. Croitoru, M. Glässl, V. M. Axt, and T. Kuhn, Phys. Rev. B **83**, 094303 (2011).

[24] M. Makhonin, J. Dixon, R. Coles, B. Royall, I. J. Luxmoore, E. Clarke, M. Hugues, M. Skolnick, and A. M. Fox, Nano letters **14**, 6997 (2014).

[25] Q. Wang, A. Muller, M. Cheng, H. Zhou, P. Bianucci, and C. Shih, Physical Review Letters **95**, 187404 (2005).

[26] R. S. Kolodka, A. J. Ramsay, J. Skiba-Szymanska, P. W. Fry, H. Y. Liu, A. M. Fox, and M. S. Skolnick, Phys. Rev. B **75**, 193306 (2007).

[27] See supplementary material.

[28] D. P. S. McCutcheon and A. Nazir, New Journal of Physics **12**, 113042 (2010).

[29] K. Roszak, V. Axt, T. Kuhn, and P. Machnikowski, Physical Review B **76**, 195324 (2007).

[30] S. Stufler, P. Machnikowski, P. Ester, M. Bichler, V. Axt, T. Kuhn, and A. Zrenner, Physical Review B **73**, 125304 (2006).

[31] We note that in single pulse experiments at 15 K, more symmetric phonon sidebands can be observed [32].

[32] A. J. Ramsay, T. M. Godden, S. J. Boyle, E. M. Gauger, A. Nazir, B. W. Lovett, A. V. Gopal, A. M. Fox, and M. S. Skolnick, J. Appl. Phys **109**, 102415 (2011).